Sub-Nyquist signal-reconstruction-free operational modal analysis and damage detection in the presence of noise

Kyriaki Gkoktsi*[a], Agathoklis Giaralis[a], Bamrung TauSiesakul[b]
[a]Dept. of Civil Engineering, City University London, Northampton Square, EC1V 0HB, London, UK; [b]Dept. of Electrical Engineering, Srinakarinwirot Prasanmitr University, 114 Sukhumvit 23, Wattana District, Bangkok 10110, Thailand

ABSTRACT

Motivated by a need to reduce energy consumption in wireless sensors for vibration-based structural health monitoring (SHM) associated with data acquisition and transmission, this paper puts forth a novel approach for undertaking operational modal analysis (OMA) and damage localization relying on compressed vibrations measurements sampled at rates well below the Nyquist rate. Specifically, non-uniform deterministic sub-Nyquist multi-coset sampling of response acceleration signals in white noise excited linear structures is considered in conjunction with a power spectrum blind sampling/estimation technique which retrieves/samples the power spectral density matrix from arrays of sensors directly from the sub-Nyquist measurements (i.e., in the compressed domain) without signal reconstruction in the time-domain and without posing any signal sparsity conditions. The frequency domain decomposition algorithm is then applied to the power spectral density matrix to extract natural frequencies and mode shapes as a standard OMA step. Further, the modal strain energy index (MSEI) is considered for damage localization based on the mode shapes extracted directly from the compressed measurements. The effectiveness and accuracy of the proposed approach is numerically assessed by considering simulated vibration data pertaining to a white-noise excited simply supported beam in healthy and in 3 damaged states, contaminated with Gaussian white noise. Good accuracy is achieved in estimating mode shapes (quantified in terms of the modal assurance criterion) and natural frequencies from an array of 15 multi-coset devices sampling at a 70% slower than the Nyquist frequency rate for SNRs as low as 10db. Damage localization of equal level/quality is also achieved by the MSEI applied to mode shapes derived from noisy sub-Nyquist (70% compression) and Nyquist measurements for all damaged states considered. Overall, the furnished numerical results demonstrate that the herein considered sub-Nyquist sampling and multi-sensor power spectral density estimation techniques coupled with standard OMA and damage detection approaches can achieve effective SHM from significantly fewer noisy acceleration measurements.

Keywords: compressive sensing, multi-coset sampling, power spectrum estimation, operational modal analysis, mode shapes, damage detection, modal strain energy.

1. INTRODUCTION

Over the past several decades, numerous algorithms for vibration-based monitoring of civil (i.e., large-scale) engineering structures and structural members have been proposed in the literature[1,2], focusing mostly on (i) estimating the dynamic/modal properties of linearly vibrating structures under operational conditions, and (ii) on detecting potential structural damage from vibration measurements. The first task is addressed by the so-called operational modal analysis (OMA) or output-only modal analysis algorithms[3] used to extract natural frequencies and mode shapes by relying on the acquisition and processing of arrays of low-amplitude acceleration response signals of structures subjected to ambient dynamic excitation (e.g., due to wind and traffic loads) not measured but modelled as broadband (white) noise. The second task involves tracing in time changes to damage sensitive indices whose definition may or may not involve physically meaningful quantities (i.e., modal and structural properties).

From the technology viewpoint, the consideration of wireless sensor networks (WSNs) attracted the attention of the research community as it is recognized that they offer less obtrusive, and more economical and rapid deployment for OMA and damage detection compared to arrays of tethered sensors[4,5], especially for the case of large scale and geometrically complex structures. However, despite the above advantages of WSNs, there are still practical issues to be overcome related to a need for local power supply at the sensors and restrictions to the amount of wireless data

*Kyriaki.Gkoktsi.1@city.ac.uk

transmission due to bandwidth limitations. To address the above issues, some recent research effort[6–10] was devoted in exploring compressive sensing (CS)-based techniques which achieve simultaneous signal acquisition and compression before transmission. In a nutshell, these techniques consider non-uniform random sampling schemes to acquire signals at an average rate below the Nyquist rate, by exploiting signal sparsity in some domain (e.g., the Fourier domain). CS asserts that exact reconstruction of the underlying Nyquist-sampled signals is guaranteed with high probability, upon solving an *underdetermined* system of linear equations subject to signal sparsity constraints. The latter is commonly formulated as a constrained ℓ_1 optimization problem whose solution is computationally costly.

In this context, *O'Connor et al.*[6] reported significant energy savings in a long-term field deployment of prototyped wireless sensors acquiring bridge acceleration response signals via a sub-Nyquist random sampling scheme based on the CS theory. Under the assumption of spectrally sparse measurements, the acquired signals are transmitted towards a base station and reconstructed to the uniform Nyquist grid by means of a standard CS signal recovery algorithm. The standard frequency domain decomposition (FDD) algorithm based on the singular value decomposition (SVD) for OMA was used to retrieve mode shapes of the considered bridge structure from the reconstructed signals. Similar CS-based acquisition and signal reconstruction steps have further been considered by *Zou et al.*[7] and *Bao et al.*[8] to address the issue of data loss during wireless transmission vibration-based health monitoring of large-scale civil engineering structures. In a different study, *Park et al.*[9] recognized that signal reconstruction from CS measurements in time-domain is not required in undertaking OMA. Therefore, they proposed a singular value decomposition based algorithm to retrieve mode shapes (but not natural frequencies) directly from sub-Nyquist non-uniform randomly sampled measurements (i.e., without signal reconstruction) assuming a deterministic multi-tone non-decaying analog signal model. Although the adopted model corresponds to non-decaying free vibration response of undamped multi-degree-of-freedom structures, the proposed approach shows robustness in extracting mode shapes from noisy field acceleration measurements of lightly-damped free vibrating structures. More recently, *Yang and Nagarajaiah*[10] coupled CS-based sampling with the blind source separation method to extract mode shapes and modal responses directly from compressed/sub-Nyquist measurements of multi-mode response vibration signals. Signal retrieval in the time-domain is then applied by means of a CS-based signal reconstruction step for each modal response to retrieve the underlying modal natural frequencies and damping ratios via standard linear system identification approaches.

All the aforementioned CS-based approaches pose signal sparsity conditions to the measured response acceleration signals, which may not hold true for noisy signals encountered in practice[11,12]. Further, response signals are treated as deterministic, which is not consistent with the theory of OMA assuming wide sense stationary stochastic input/excitation processes. Further, with the exception of the work by *Park et al.*[9], all the above CS methods require computational expensive CS-based signal reconstruction from the compressed (sub-Nyquist) measurements upon wireless transmission.

This paper builds on recent work by the authors[13–16] to accomplish OMA and damage detection directly from compressed measurements of response acceleration stochastic processes (i.e., without signal reconstruction in the time-domain), and without posing any sparsity conditions by means of sub-Nyquist power spectrum blind sampling (PSBS). In particular, PSBS strategies aims to reconstruction of the covariance function of random signals or stochastic processes at all temporal lags of interest. This operation leads to an overdetermined optimization problem which can be solved with standard ℓ_2 minimization algorithms. Further, it has been shown that PSBS are suitable for spectral recovery of very weak compressed signals buried in high level noise[12,17]. In this respect, the proposed approach is based on non-uniform deterministic multi-coset sampling[18,19] along with a particular PSBS method[13–15]. The adopted method approach was first considered by the authors[14,15] for single-sensor spectrum estimation, showing promising results in retrieving the frequency response function of white-noise excited multi-degree-of-freedom systems. Herein, the multi-sensor case[16] is employed to estimate the cross-power spectral density matrix directly from sub-Nyquist sampled structural response signals within a centralized cooperative WSN. The thus obtained matrix is used along with the FDD algorithm[20], to retrieve the underlying structural modal properties (natural frequencies, mode shapes). Further, the extracted mode shapes are used for structural damage detection based on the modal strain energy index (MSEI)[21].

The remainder of the paper is organized as follows: Section 2 outlines the theory of the adopted multi-coset sub-Nyquist sampling and PSBS technique, Section 3 reviews the FDD algorithm for OMA and the MSEI for damage localization in linear frame/flexural structures, Section 4 furnishes numerical results pertaining to simulated response acceleration data to illustrate the applicability and effectiveness of the proposed approach for modal identification and damage detection, and Section 5 summarizes concluding remarks.

2. SUB-NYQUIST SAMPLING STRATEGY AND BLIND SPECTRUM ESTIMATION

2.1 Multi-coset sampling pattern and device

Let $x(t)$ be a continuous in time t real-valued wide-sense stationary random signal (or stochastic process) characterized in the frequency domain by the power spectrum $P_x(\omega)$ band-limited by $2\pi/T$. It is desired to sample $x(t)$ at a rate lower than the Nyquist sampling rate $1/T$ (in Hz), and still be able to obtain a useful estimate of the power spectrum $P_x(\omega)$. To this aim, a multi-coset sampling strategy is herein adopted[19], according to which the uniform grid of Nyquist sampled measurements $x(nT)= x[n]$, n=0,1,2,… is first divided into blocks of N consecutive samples. Then, from each block, a number of M samples ($M<N$) are selected having the same pre-defined position for all blocks. Therefore, the adopted sampling strategy yields non-uniform in time, deterministically selected N-periodic samples and can be implemented by utilizing M interleaved analog to digital converters (ADCs) operating at a sampling rate $1/(NT)$. A discrete-time model of such a multi-coset sampling device discussed in Arianandа and Leus[18] is shown in Figure 1 in which the discrete-time signal $x[n]$ enters M channels and at each m channel (m= 0,1,…,M-1), the signal is convolved (filtered) by an N-length sequence $c_m[n]$ and down-sampled by N.

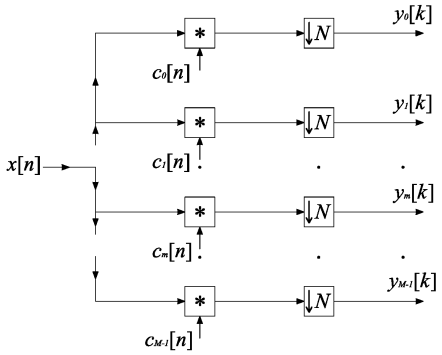

Figure 1. Discrete-time model of the adopted sampling device[18].

The selection of M samples within each N-length block is defined by the sampling sequence (or sampling pattern)

$$\mathbf{n} = [n_0 \quad n_1 \quad \cdots \quad n_{M-1}]^{\mathrm{T}}, \tag{1}$$

and is governed by the filter coefficients $c_m[n]$ written as

$$c_m[n] = \begin{cases} 1, & n = -n_m, \\ 0, & n \neq -n_m, \end{cases} \tag{2}$$

where there is no repetition in n_m, i.e.,

$$n_{m_i} \neq n_{m_j}, \quad \forall\ m_i \neq m_j. \tag{3}$$

The output of the m-th channel is given by

$$y_m[k] = \sum_{p=1-N}^{0} c_m[p]\ x[kN - p]. \tag{4}$$

2.2 Input/ Output Cross-Correlation Function Relationships

Consider an array of D identical sub-Nyquist multi-coset sampling devices recording the acceleration response at different locations of a white noise excited structure. Each device has M channels with output sequences $y_m^d[l]$ where

m= 0,1,…, M−1 and d=1, 2,…, D. The cross-correlation function between two output sequences of the m_i channel of the d_a device and of the m_j channel of the d_b device is hereafter denoted by

$$r_{y_i^a, y_j^b}[k] = \mathrm{E}_y\left\{ y_{m_i}^{d_a}[l]\, y_{m_j}^{d_b}[l-k] \right\}, \tag{5}$$

where $E_a\{\cdot\}$ is the mathematical expectation operator with respect to a. Further, the cross-correlation function between the input signals $x^d[m]$ to the devices d_a and d_b is denoted by

$$r_{x^a x^b}[n] = \mathrm{E}_x\left\{ x^{d_a}[m]\, x^{d_b}[m-n] \right\}. \tag{6}$$

To reduce communication overhead and computational complexity of sensors, it is assumed that all considered devices have the same sampling pattern across their channels within a signal-and-structure-agnostic sensing framework. Under this assumption, the common pattern cross-correlation function is expressed as

$$r_{c_i, c_j}[n] = \sum_{k=1-N}^{0} c_{m_i}[k]\; c_{m_j}[k-n] = \delta[n-(n_{m_i} - n_{m_j})], \tag{7}$$

where $\delta[n]$ = 1 for n = 0 and $\delta[n]$ = 0 for $n \neq 0$. Further, the above assumption allows to relate the cross-correlation functions of the output sequences in the array of devices as

$$\mathbf{r}_{y^a y^b}[k] = \sum_{l=0}^{1} \mathbf{R}_c[l]\; \mathbf{r}_{x^a x^b}[k-l], \tag{8}$$

which is a generalization of the previously considered in the literature single-sensor case[13–15,18]. In the last equation,

$$\mathbf{r}_{y^a y^b}[k] = \left[r_{y_0^a, y_0^b}[k] \;\cdots\; r_{y_0^a, y_{(M-1)}^b}[k] \quad r_{y_1^a, y_0^b}[k] \;\cdots\; r_{y_{(M-1)}^a, y_{(M-1)}^b}[k] \right]^{\mathrm{T}} \tag{9}$$

is the M^2-by-D matrix collecting the output cross-correlation sequences $r_{y_i^a, y_j^b}[k]$ among the M channels of the devices array, where "T" subscript denotes matrix transposition;

$$\mathbf{r}_{x^a x^b}[n] = \left[r_{x^a x^b}[nN] \quad r_{x^a x^b}[nN+1] \;\cdots\; r_{x^a x^b}[(n+1)N-1] \right]^{\mathrm{T}}. \tag{10}$$

is the N-by-D matrix collecting the input cross-correlation sequences; and $\mathbf{R}_c[l]$ is the M^2-by-N matrix defined as

$$\mathbf{R}_c[l] = \left[\mathbf{r}_{c_0, c_0}[l] \;\cdots\; \mathbf{r}_{c_0, c_{M-1}}[l] \quad \mathbf{r}_{c_1, c_0}[l] \;\cdots\; \mathbf{r}_{c_{M-1}, c_{M-1}}[l] \right]^{\mathrm{T}}. \tag{11}$$

By assuming that the input cross-correlation sequences $\mathbf{r}_{x^a x^b}[n]$ take on negligible values outside the range $-L \le k \le L$, the input/output relationship can be cast in matrix form

$$\mathbf{r}_{y^a y^b} = \mathbf{R}_c \mathbf{r}_{x^a x^b}, \tag{12}$$

where $\mathbf{r}_{y^a y^b}$ is the $M^2(2L+1)$-by-D matrix defined as

$$\mathbf{r}_{y^a y^b} = \left[\mathbf{r}^{\mathrm{T}}_{y^a y^b}[0] \;\cdots\; \mathbf{r}^{\mathrm{T}}_{y^a y^b}[L] \quad \mathbf{r}^{\mathrm{T}}_{y^a y^b}[-L] \;\cdots\; \mathbf{r}^{\mathrm{T}}_{y^a y^b}[-1] \right]^{\mathrm{T}}, \tag{13}$$

$\mathbf{r}_{x^a x^b}$ is the $N(2L+1)$-by-D matrix defined in a similar manner as $\mathbf{r}_{y^a y^b}$, and $\mathbf{R}_c$ is the $M^2(2L+1)$-by-$N(2L+1)$ matrix given as

$$\mathbf{R}_{\mathrm{c}} = \begin{bmatrix} \mathbf{R}_c[0] & \mathbf{O} & \cdots & \mathbf{O} & \mathbf{R}_c[1] \\ \mathbf{R}_c[1] & \mathbf{R}_c[0] & \mathbf{O} & \ddots & \mathbf{O} \\ \mathbf{O} & \mathbf{R}_c[1] & \mathbf{R}_c[0] & \ddots & \vdots \\ \vdots & \ddots & \ddots & \ddots & \mathbf{O} \\ \mathbf{O} & \cdots & \mathbf{O} & \mathbf{R}_c[1] & \mathbf{R}_c[0] \end{bmatrix}, \tag{14}$$

Note that Eq. (12) defines an overdetermined system of linear equations which can be solved for $\mathbf{r}_{y^a y^b}$ without any sparsity constraints provided that $\mathbf{R}_{\mathrm{c}}$ is full column rank. The latter condition is satisfied for $M^2 \geq N$.

2.3 Power Spectrum Blind Sampling from sub-Nyquist measurements

Suppose that $x^a[n]$ and $x^b[n]$ are sampled at the Nyquist rate from the band-limited continuous-time processes $x^a(t)$ and $x^b(t)$ respectively. The cross power spectrum of $x^a(t)$ and $x^b(t)$ can be expressed within the $0 \leq \omega \leq 2\pi$ range as

$$P_{x^a x^b}(\omega) = \sum_{n=-\infty}^{\infty} r_{x^a x^b}[n]\, \mathrm{e}^{-\mathrm{i}n\omega}, \tag{15}$$

where $i = \sqrt{-1}$. The latter expression is further discretized in the frequency domain and cast in matrix form

$$\mathbf{s}_{x^a x^b} = \mathbf{F}_{(2L+1)N} \mathbf{r}_{x^a x^b}, \tag{16}$$

where $\mathbf{F}_{(2L+1)N}$ is the $N(2L+1)$-by-$N(2L+1)$ standard discrete Fourier transform (DFT) matrix and $\mathbf{s}_{x^a x^b}$ is a $N(2L+1)$-by-D power spectrum matrix computed at the discrete frequencies $\omega = [0, 2\pi/((2L+1)N), \ldots, 2\pi(2L+1)N-1/((2L+1)N)]$.

Consider the unbiased estimator of the output cross-correlation function

$$\hat{r}_{y_i^a, y_j^b}[k] = \frac{1}{K - |k|} \sum_{l=\max\{0,k\}}^{K-1+\min\{0,k\}} y_{m_i}^{d_a}[l]\, y_{m_j}^{d_b}[l-k]. \tag{17}$$

The following weighted least square criterion is herein adopted

$$\hat{\mathbf{r}}_{x^a x^b} = \arg\min_{\mathbf{r}_{x^a x^b}} \left\| \hat{\mathbf{r}}_{y^a y^b} - \mathbf{R}_{\mathrm{c}} \mathbf{r}_{x^a x^b} \right\|_{\mathbf{W}}^2, \tag{18}$$

in which the weighted version of the Euclidean norm is given by $\|\mathbf{a}\|_{\mathbf{W}}^2 = \mathbf{a}^T \mathbf{W} \mathbf{a}$, and $\mathbf{W}$ is a weighting matrix. An estimate of the cross-spectrum matrix $\mathbf{s}_{x^a x^b}$ is obtained by

$$\hat{\mathbf{s}}_{x^a x^b} = \mathbf{F}_{(2L+1)N} \left(\mathbf{R}_c^{\mathrm{T}} \mathbf{W}^{-1} \mathbf{R}_c \right)^{-1} \mathbf{R}_c^{\mathrm{T}} \mathbf{W}^{-1} \hat{\mathbf{r}}_{y^a y^b}, \tag{19}$$

where the "−1" superscript denotes matrix inversion. The cross-spectrum matrix in Eq. (19) is efficiently computed directly from the cross-correlation estimator $\hat{\mathbf{r}}_{y^a y^b}$ of the compressed acceleration measurements from the array of D sampling devices. This is achieved by exploiting the sparse structure of $\mathbf{R}_{\mathrm{c}}$ as detailed in[13].

3. OPERATIONAL MODAL ANALYSIS AND DAMAGE DETECTION STEPS

3.1 Sub-Nyquist operational modal analysis using the frequency domain decomposition (FDD) algorithm

In this work, the standard frequency domain decomposition (FDD) algorithm[20] is employed, out of the numerous frequency domain algorithms for OMA found in the literature, to retrieve the structural modal properties from the cross-

spectral matrix in Eq. (19). In a nutshell, the FDD algorithm relies on the singular value decomposition of the cross-spectral matrix $\hat{\mathbf{s}}_{x^a x^b}$, that is,

$$\hat{\mathbf{s}}_{x^a x^b} = \mathbf{U}\boldsymbol{\Sigma}\mathbf{V}^{\mathrm{T}} \tag{20}$$

where $\boldsymbol{\Sigma}$ is a diagonal positive semi-definite matrix populated by the singular values, and $\mathbf{U}$, $\mathbf{V}$ are the unitary singular matrices collecting the left and right singular vectors respectively. The dominant (largest) singular values carry the information of the excited natural frequencies of the vibrating structure. Further, the pertinent mode shapes are extracted from the left singular vector $\mathbf{U}$ corresponding to the dominant singular values. More details on the FDD algorithm can be found in a recent text[3] and in the therein references. For the purposes of this study, it is important to note that the herein proposed OMA approach retrieves both the mode shapes and the natural frequencies from the cross-spectral matrix in Eq.(19) estimated directly from the sub-Nyquist (compressed measurements). No acceleration signals reconstruction (i.e. retrieval of the $x[n]$ input sequences to the considered array of sensors), and, more generally, no solution of any ℓ_1 optimization problem is undertaken for the task as required by other recent compressive sensing based OMA approaches proposed in the literature[6,10].

3.2 Sub-Nyquist structural damage detection using the modal strain energy index (MSEI)

Upon retrieval of the structural mode shapes, a further step is herein pursued towards vibration-based structural health monitoring of civil engineering structures directly from sub-Nyquist/compressed acceleration measurements acquired under operational conditions. To this aim, the modal strain energy index (MSEI)[21] is adopted to achieve structural damage localization by relying on the mode shapes of a reference (healthy) state and of a potentially damaged state of a given structure derived from sub-Nyquist acceleration data as discussed in the previous sub-section. Focusing on rigid-jointed frame structures, the computation of the MSEI requires dividing each structural member into Z number of segments along the local longitudinal axis u defined by the $[u_z, u_{z+1}]$ intervals with $z=1,2,\ldots,Z$ and $u_1=0$, $u_{Z+1}=\lambda$, with λ being the length of the structural member. Under the assumption that at the damaged state, damage is localized within a few segments and, therefore, (i) the flexural rigidity of structural members of the healthy structure EI is equal to the flexural rigidity of structural members of the damaged structure EI^*, and (ii) the strain energy stored due to modal deformation for each mode shape is also equal between the healthy and the damaged states, the MSEI is defined by the ratio[21,22]

$$\beta_z = \frac{1+\sum_{r=1}^{R}\left[\int_{u_z}^{u_{z+1}}\left(\frac{\partial^2\varphi_r^*}{\partial u^2}\right)^2 du \Big/ \int_0^{\lambda}\left(\frac{\partial^2\varphi_r^*}{\partial u^2}\right)^2 du\right]}{1+\sum_{r=1}^{R}\left[\int_{u_z}^{u_{z+1}}\left(\frac{\partial^2\varphi_r}{\partial u^2}\right)^2 du \Big/ \int_0^{\lambda}\left(\frac{\partial^2\varphi_r}{\partial u^2}\right)^2 du\right]}. \tag{21}$$

The above index achieves damage localization by detecting local changes to the flexural rigidity within each segment between the healthy and the damaged states. The flexural rigidities are computed from the modal curvatures (i.e., second derivative of the mode shapes) of the first R excited modes denoted by $\varphi_r(u)$ and $\varphi^*_r(u)$, $r=1,2,\ldots,R$ for the healthy and the damaged structure, respectively. Therefore, the MSEI quantifies potential local stiffness reduction inferring damage in small segments of structures based on the differences of the first R modal curvatures or, equivalently, mode shapes. In the ensuing numerical work, the following normalized version of the MSEI is reported

$$\bar{\beta}_z = \frac{\beta_z - \mu_\beta}{\sigma_\beta}, \tag{22}$$

where μ_β is the mean, and σ_β the standard deviation of the MSEI computed across all considered segments. The damage index in Eq. (22) yields positives values at the damaged locations of the considered structure and negative values elsewhere. Overall, the MSEI is suitable when only incomplete modal information is available (e.g. only few mode shapes are excited)[21], while there is no requirement on the normalization (mass, displacement, etc.) of the considered mode shapes[23]. Although it may overestimate damage severity[21], it is shown to be a quite reliable damage index[22] especially in case of noisy data[24].

4. NUMERICAL APPLICATION

4.1 Finite Element (FE) modeling, response history analysis, and power spectrum blind estimation

For numerical verification of the proposed approach, simulated acceleration data are generated by undertaking linear response history analyses for finite element (FE) models of a simply supported IPE300-profiled steel beam at one healthy and three different damage states. The considered beam, shown in Figure 2, has length λ=5m and flexural rigidity EI=16.78·10^3 kNm^2 (i.e., elastic modulus E=210 GPa, moment of inertia around the z-axis I=7.99·10^{-5} m^4). It is modelled in the commercial FE software SAP2000 using 100 Euler-Bernoulli beam elements of equal length with mass lumped at the nodes of the FE grid acting along the gravitational z-axis. It is assumed that the beam is instrumented with an array of 15 sensors distributed along the beam length with locations marked by an "x" in Figures 2 and 3. Three different damaged states of increasing severity are defined by local stiffness reduction close to mid-span of 50% within a 0.1m width (damage state *DS1*), of 50% within a 0.2m width (damage state *DS2*), and of 80% within a 0.2m width (damage state *DS3)*, as shown in Figure 3.

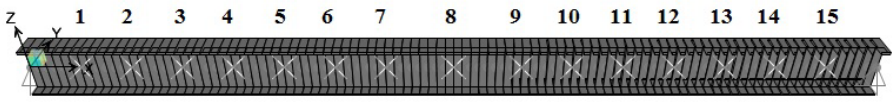

Figure 2. Simply supported steel beam instrumented with 15 sampling devices measuring vertical acceleration response signals.

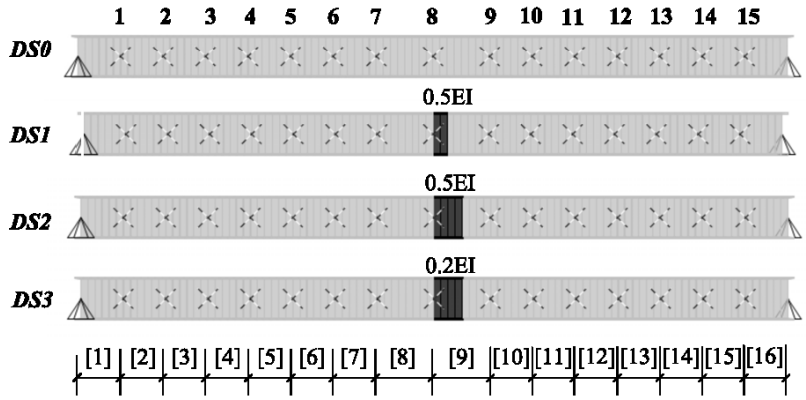

Figure 3. Damage states; *DS0*: intact/healthy structure; *DS1*: 50% stiffness reduction over 0.1m beam length; *DS2*: 50% stiffness reduction over 4 beam element; *DS3*: 80% stiffness reduction over 4 beam element.

Linear response history analysis is undertaken for the FE models of the above 3 damage states and of the healthy/reference state *DS0* subjected to a low-amplitude Gaussian white noise base-excitation along the gravitational axis of 4s duration with time discretization step 0.0005s, corresponding to a Nyquist frequency of 1000Hz. A critical damping ratio of 1% for all modes of vibration is assumed in the analysis, and the vertical acceleration response signals are recorded at a sampling rate of 2000Hz (i.e., 8000 "Nyquist measurements" per signal) at the 15 points of the FE grid where the sampling devices of the considered array of sensors are deployed. The considered excitation is assumed to simulate ambient noise input under operational conditions. It excites the first three bending modes of vibration along the gravitational direction of the different states of the simply supported beam. Consequently, the obtained response acceleration signals are treated as typical noise-free vibration/acceleration data for OMA.

Next, these signals are contaminated with additive Gaussian white noise at 3 different signal-to-noise ratios (*SNRs*): 10^{20}db (i.e., practically noise-free case), 20db, and 10db (extreme noise case). The noisy acceleration response signals $x^d[n]$, (d=1,2,…,15), are multi-coset sampled by the device shown in Figure 1 assumed to have the same specifications for all 15 wireless sensors: number of channels M=5 channels and downsampling parameter N=16, achieving a compression ratio of M/N $\simeq$ 31%. That is, only 8000*5/16= 2500 (compressed) measurements y^d[k] are acquired by each of the 15 sensors out of the 8000 Nyquist samples. The adopted sampling pattern in Eq. (1) is $\boldsymbol{n}$=[0 1 2 5 8]^T. This

sequence is optimal in the mean square sense and has been derived by solution of a properly defined optimization problem[13,15]. Lastly, Eq. (18) is employed to derive the unbiased estimator of the cross-correlation matrix, $\hat{\mathbf{r}}_{y^a y^b}$ (a,b=1,2,…,15), which is subsequently used in Eq. (19) to approximate the underline cross-spectra $\hat{\mathbf{s}}_{x^a x^b}$ in the compressed domain, without any signal reconstruction operation, for the healthy *DS0* and the three damaged states *DS1-DS3*.

4.2 Operational modal analysis results

The FDD algorithm in sub-section 3.1 is applied to the estimated acceleration response spectrum matrix $\hat{\mathbf{s}}_{x^a x^b}$ to extract the modal properties of the 4 considered structural states *DS0-DS3*, for the three *SNR*s. The natural frequencies f_1 to f_3 retrieved from the largest singular values in Eq.(20) corresponding to the first three vertical vibration modes from all structural states of the considered beam are reported in Tables 1 and 2 for the noiseless (*SNR*=10^{20}dB) and extreme noisy (*SNR*=10dB) cases, respectively. In both tables, estimates of the natural frequencies obtained from the Nyquist measurements using conventional cross-spectral estimation and the FDD algorithm are also reported. It is seen that the noise level does not significantly affect the natural frequency estimation in this particular case. More importantly, the estimated natural frequencies extracted directly from the sub-Nyquist measurements by means of the proposed OMA approach lie very close to the estimates obtained from the Nyquist measurements (maximum observed error is 4.4%). As expected, the value of the natural frequencies decreases with increasing damage severity and this change in the values is more significant for natural frequencies corresponding to higher modes of vibration.

Table 1. Nyquist FDD versus sub-Nyquist FDD for natural frequency estimation at *DS0-DS3* for *SNR*=10^{20} dB.

	f_1 [Hz]		***f_2 [Hz]***		***f_3 [Hz]***	
	Nyquist (8000 samples)	*sub-Nyquist (2500 samples)*	*Nyquist (8000 samples)*	*sub-Nyquist (2500 samples)*	*Nyquist (8000 samples)*	*sub-Nyquist (2500 samples)*
DS0	40.04	39.76	310.55	311.93	717.77	718.65
DS1	39.06	39.76	310.55	311.93	716.80	712.54
DS2	38.09	39.76	302.73	305.81	704.10	712.54
DS3	35.16	33.64	288.09	287.46	676.76	678.90

Table 2. Nyquist FDD versus sub-Nyquist FDD for natural frequency estimation at *DS0-DS3* for *SNR*=10 dB.

	f_1 [Hz]		***f_2 [Hz]***		***f_3 [Hz]***	
	Nyquist (8000 samples)	*sub-Nyquist (2500 samples)*	*Nyquist (8000 samples)*	*sub-Nyquist (2500 samples)*	*Nyquist (8000 samples)*	*sub-Nyquist (2500 samples)*
DS0	40.04	39.76	310.55	311.93	717.77	718.65
DS1	39.06	39.76	310.55	311.93	704.10	712.54
DS2	38.09	39.76	302.73	305.81	704.10	712.54
DS3	35.16	33.64	288.09	287.46	676.76	678.90

Moreover, Figure 4 plots the first three vertical modes of vibration for the healthy beam state derived from both the Nyquist (8000 measurements/sensor) and sub-Nyquist/compressed (2500 measurements/sensor) data for *SNR*=10dB. These mode shapes are retrieved from the left singular vector **U** of the decomposed spectral matrix in Eq. (20). It is seen that the estimated modes retrieved from about 70% less measurements from Nyquist sampling are visually close to the estimated ones from the Nyquist measurements.

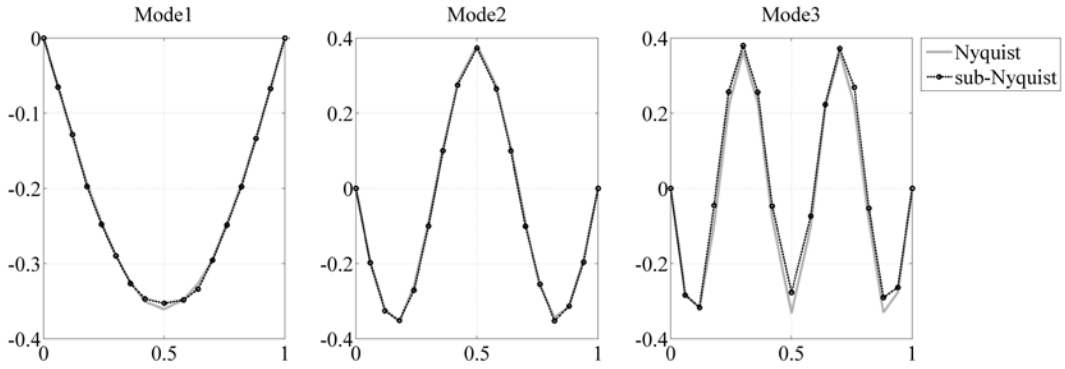

Figure 4. Nyquist FDD versus sub-Nyquist FDD for mode shape estimation at *DS0* for *SNR=10dB* (the horizontal axis gives the relative distance from the left support of the beam normalized with its length).

To quantify the level of accuracy for the extracted mode shapes, the modal assurance criterion (*MAC*)[25]

$$MAC(\varphi,\hat{\varphi}) = \frac{\left|\varphi^{\mathrm{T}}\hat{\varphi}\right|^2}{\left\|\varphi\right\|_2^2 \left\|\hat{\varphi}\right\|_2^2} \tag{23}$$

is considered which measures the statistical correlation between the modes shapes, $\hat{\varphi}$ and φ, corresponding to mode shapes estimated by means of the FDD algorithm from sub-Nyquist and Nyquist samples, respectively. The normalized inner product in Eq. (23) yields a scalar value within the range of [0, 1] and values of 0.9 and higher suggests acceptable overall similarity/proximity between the $\hat{\varphi}$ and φ vectors. Tables 3 and 4 report MAC values for the first three modes of vibration for all structural states of the beam considered (*DS0-DS3*) and for *SNR*=10^{20} dB and *SNR*=10dB noise levels, respectively. Most of the MAC values in Tables 3 and 4 are close to unity, demonstrating a high level of correlation between the estimated mode shapes $\hat{\varphi}$ and φ and confirming the good accuracy of the proposed sub-Nyquist OMA approach. In fact, MAC drops below 0.9 only in the case of the third mode shape of the *DS1*. Finally, a comparison between Table 3 and Table 4 confirms that the obtained mode shape estimates from sub-Nyquist measurements are not sensitive to additive Gaussian white noise.

Table 3. Modal Assurance Criterion (sub-Nyquist FDD versus Nyquist FDD) on the estimated mode shapes at *DS0-DS3* for *SNR*=10^{20} dB.

	MAC 1st mode	***MAC 2nd mode***	***MAC 3rd mode***
	sub-Nyquist/Nyquist	*sub-Nyquist/Nyquist*	*sub-Nyquist/Nyquist*
DS0	1.000	0.999	0.987
DS1	0.999	0.999	0.888
DS2	0.998	0.996	0.988
DS3	0.999	0.999	0.995

Table 4. Modal Assurance Criterion (sub-Nyquist FDD versus Nyquist FDD) on the estimated mode shapes at *DS0-DS3* for *SNR*=10 dB.

	MAC 1st mode	***MAC 2nd mode***	***MAC 3rd mode***
	sub-Nyquist/Nyquist	*sub-Nyquist/Nyquist*	*sub-Nyquist/Nyquist*
DS0	1.000	0.999	0.984
DS1	0.999	0.999	0.852
DS2	0.997	0.995	0.990
DS3	0.999	0.999	0.991

4.3 Damage localization results

In this section, the potential of using the MSEI described in sub-section 3.2 for damage localization from mode shapes estimated directly from sub-Nyquist measurements is numerically illustrated. To this aim, the normalized damage index $\overline{\beta}_z$ in Eq. (22) is computed from the estimated mode shapes, $\varphi_{DS0}, \varphi^*_{DS1}, \varphi^*_{DS2}, \varphi^*_{DS3}$ corresponding to the healthy (*DS0*) and damaged states (*DS1-DS3*) respectively, upon dividing the beam in Figure 3 in Z=16 segments. The second derivatives appearing in Eq. (21) are numerically approximated with the standard finite difference method. The location of damage is inferred by the positive amplitudes of the normalized damage index $\overline{\beta}_z$ plotted in Figures 5, 6, and 7 for SNR=10^{20} dB, SNR=20dB and SNR=10dB, respectively obtained from both Nyquist measurements (left figure panels) and sub-Nyquist measurements (right figure panels). It is seen that for the *DS2* and *DS3* states, the MSEI computed from the sub-Nyquist measurements can unambiguously identify the damage location (mid-span) and even discern the damage severity for *SNR* as low as 10db. In fact, the MSEI derived from sub-Nyquist measurements performs equally well with the MSEI from Nyquist measurements, although 70% fewer measurements are used in mode shape estimation. In the case of the least severe damaged state herein considered, *DS1*, the MSEI computed by the proposed approach performs relatively well in locating damage for the noise-less case. For noisy sub-Nyquist measurements, discriminating damage location becomes challenging (see right panel in Figure 6) for SNR=20db and practically not possible for SNR= 10db. Note, however, that this is pretty much the case for the MSEI obtained for Nyquist sampled measurements and, therefore, the fact that the MSEI cannot accurately and unambiguously locate the damage from noisy signals for the *DS1* case is a matter of the effectiveness of the particular damage index to locate relatively small damages and well-localized damage in noisy environments, rather than damage information loss due to the sub-Nyquist signal sampling.

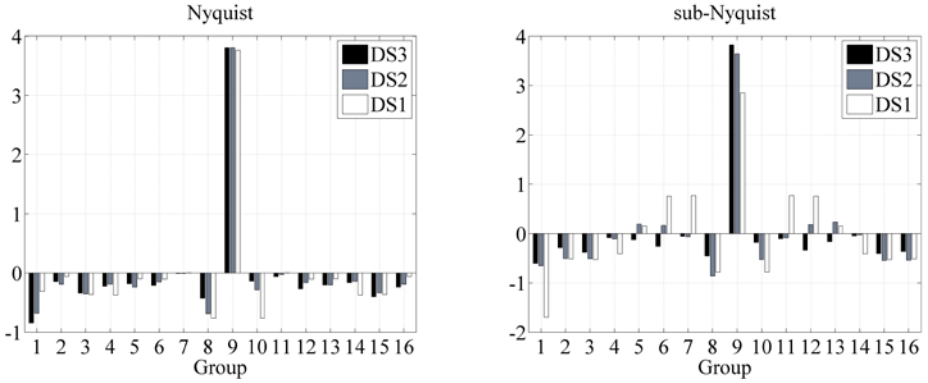

Figure 5. Nyquist (left) and sub-Nyquist (right) normalized modal strain energy index for *DS0-DS3*for SNR=10^{20}dB.

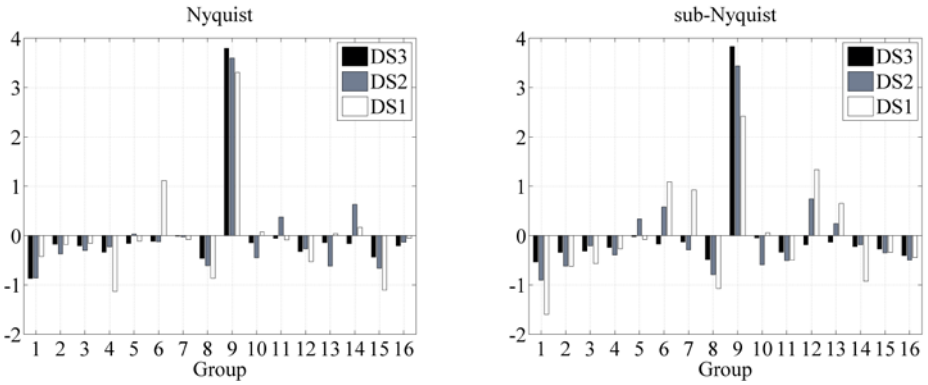

Figure 6. Nyquist (left) and sub-Nyquist (right) normalized modal strain energy index for *DS0-DS3* for SNR=20dB.

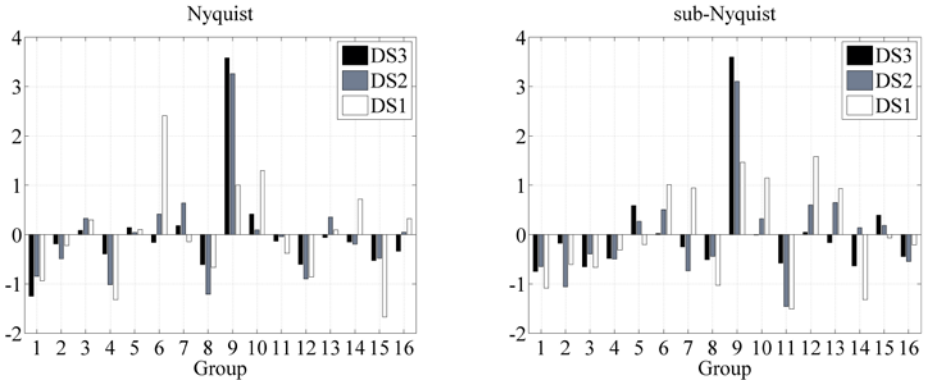

Figure 7. Nyquist (left) and sub-Nyquist (right) normalized modal strain energy index for *DS0-DS3* for *SNR*=10dB.

5. CONCLUDING REMARKS

Motivated by a need to reduce energy consumption in wireless sensors for vibration-based structural health monitoring (SHM) associated with data acquisition and transmission, this work considered an approach for undertaking operational modal analysis (OMA) and damage localization relying on compressed vibrations measurements sampled at rates well below the Nyquist rate. Specifically, non-uniform deterministic sub-Nyquist multi-coset sampling of response acceleration signals in white noise excited linear structures has been considered in conjunction with a power spectrum estimation technique which retrieves/samples the power spectral density matrix from arrays of sensors directly from the sub-Nyquist measurements (i.e., in the compressed domain) without signal reconstruction in the time-domain and without posing any signal sparsity conditions. The frequency domain decomposition algorithm is then applied to the power spectral density matrix to extract natural frequencies and mode shapes as a standard OMA step. Further, the modal strain energy index (MSEI) was considered for damage localization based on the mode shapes extracted directly from the compressed measurements. The applicability and effectiveness of the proposed SHM approach based on compressed/sub-Nyquist output-only acceleration measurements has been numerically assessed by considering simulated vibration data pertaining to a white-noise excited simply supported beam in healthy and 3 damaged states, contaminated with Gaussian white noise. The first three mode shapes of the healthy beam have been estimated from an array of 15 multi-coset devices sampling at a 70% slower than the Nyquist frequency rate, with MAC values well above 0.90 compared to the mode shapes retrieved from Nyquist sampled signals and for SNRs as low as 10db. Moreover, the associated natural frequencies were estimated directly from the noisy compressed measurements with an error of less than 4.5%. Finally, damage localization of equal level/quality has been achieved by the MSEI applied to mode shapes derived from Nyquist and the sub-Nyquist (70% fewer) measurements for all damaged states considered and SNRs. Overall, the furnished numerical results demonstrate that the herein considered sub-Nyquist sampling and multi-sensor power spectral density estimation techniques coupled with standard OMA and damage detection approaches can achieve effective SHM from significantly fewer acceleration measurements even in noisy environments. Further numerical work involving more complex structures, field measurements, and higher compression ratios is undertaken by the authors to establish the limits of accuracy of the proposed compressed/sub-Nyquist based approach for OMA and damage detection.

ACKNOWLEGMENTS

This work has been funded by EPSRC in UK, under grant No EP/K023047/1. The first author acknowledges the support of City University London through a PhD studentship.

REFERENCES

[1] Doebling, S. W., Farrar, C. R., Prime, M. B., “A summary Review of Vibration-Based Damage ldentification Methods,” Shock Vib. Dig. 30(2), 91–105 (1988).

[2] Sohn, H., Farrar, C. R., Hemez, F., Czarnecki, J., “A Review of Structural Health Monitoring Literature 1996 – 2001,” Third World Conf. Struct. Control(DECEMBER), 1–7 (2002).

[3] Brincker, R., Ventura, C. E., [Introduction to Operational Modal Analysis], John Wiley & Sons, (2015).

[4] Lynch, J. P., “An overview of wireless structural health monitoring for civil structures,” Philos. Trans. R. Soc. A Math. Phys. Eng. Sci. 365(1851), 345–372 (2007).

[5] Spencer, B. F. J., Yun, C.B., “Wireless Sensor Advances and Applications for Civil Infrastructure Monitoring,” Newmark Structural Engineering Laboratory University of Illinois at Urbana-Champaign, (2010).

[6] O’Connor, S. M., Lynch, J. P., Gilbert, A. C., “Compressed sensing embedded in an operational wireless sensor network to achieve energy efficiency in long-term monitoring applications,” Smart Mater. Struct. 23(8), 085014, IOP Publishing (2014).

[7] Zou, Z., Bao, Y., Li, H., Spencer, B. F., Ou, J., “Embedding compressive sensing-based data loss recovery algorithm into wireless smart sensors for structural health monitoring,” IEEE Sens. J. 15(2), 797–808 (2015).

[8] Bao, Y., Li, H., Sun, X., Yu, Y., Ou, J., “Compressive sampling-based data loss recovery for wireless sensor networks used in civil structural health monitoring,” Struct. Heal. Monit. 12(1), 78–95 (2013).

[9] Park, J. Y., Wakin, M. B., Gilbert, A. C., “Modal analysis with compressive measurements,” IEEE Trans. Signal Process. 62(7), 1655–1670 (2014).

[10] Yang, Y., Nagarajaiah, S., “Output-only modal identification by compressed sensing: Non-uniform low-rate random sampling,” Mech. Syst. Signal Process. 56-57, 15–34, Elsevier (2015).

[11] Davenport, M. A., Laska, J. N., Treichler, J. R., Baraniuk, R. G., “The Pros and Cons of Compressive Sensing for Wideband Signal Acquisition: Noise Folding versus Dynamic Range,” IEEE Trans. Signal Process. 60(9), 4628–4642 (2012).

[12] Axell, E., Leus, G., Larsson, E., Poor, H., “Spectrum Sensing for Cognitive Radio : State-of-the-Art and Recent Advances,” IEEE Signal Process. Mag. 29(3), 101–116 (2012).

[13] Tausiesakul, B., Gonzalez-Prelcic, N., “Power Spectrum Blind Sampling Using Minimum Mean Square Error and Weighted Least Squares,” 47th Asilomar Conf. Signals, Syst. Comput. (ACSSC), 153–157 (2013).

[14] Tausiesakul, B., Gkoktsi, K., Giaralis, A., “Compressive Sensing Spectral Estimation For Output-Only Structural System Identidication,” 7th Int. Conf. Comput. Stoch. Mech., 1–12 (2014).

[15] TauSiesakul, B., Gkoktsi, K., Giaralis, A., “Compressive power spectrum sensing for vibration-based output-only system identification of structural systems in the presence of noise,” SPIE Sens. Technol. + Appl.(i), (2015).

[16] Gkoktsi, K., TauSiesakul, B., Giaralis, A., “Multi-channel sub-Nyquist cross-Spectral Estimation for Modal Analysis of Vibrating Structures,” Int. Conf. Syst. Signals Image Process. (IWSSIP 2015), (2015).

[17] Arianandа, D. D., Leus, G., “Cooperative compressive wideband power spectrum sensing,” 2012 Conf. Rec. Forty Sixth Asilomar Conf. Signals, Syst. Comput., 303–307, IEEE (2012).

[18] Arianandа, D. D., Leus, G., “Compressive Wideband Power Spectrum Estimation,” Signal Process. IEEE Trans. 60(9), 4775–4789 (2012).

[19] Mishali, M., Eldar, Y. C., “Blind Multiband Signal Reconstruction: Compressed Sensing for Analog Signals,” IEEE Trans. Signal Process. 57(3), 993–1009 (2009).

[20] Brincker, R., Zhang, L., Andersen, P., “Modal identification from ambient responses using frequency domain decomposition,” Proc. Int. Modal Anal. Conf. - IMAC 1, 625–630, SEM (2000).

[21] Kim, J.-T., Stubbs, N., “Damage Detection In Offshore Jacket Structures From Limited Modal Information,” Int. J. Offshore Polar Eng. 5(01), International Society of Offshore and Polar Engineers (1995).

[22] Humar, J., “Performance of Vibration-based Techniques for the Identification of Structural Damage,” Struct. Heal. Monit. 5(3), 215–241 (2006).

[23] Cornwell, P., Doebling, S. W., Farrar, C. R., “Application of the Strain Energy Damage Detection Method To Plate-Like Structures,” J. Sound Vib. 224(2), 359–374 (1999).

[24] Alvandi, A., Cremona, C., “Assessment of vibration-based damage identification techniques,” J. Sound Vib. 292(1-2), 179–202 (2006).

[25] Ewins, D. J., [Modal testing], Research Studies Press, (2000).